

A Premixed Jet Flame behind a Conical Bluff Body: Its MILD Combustion Characteristics versus the Conventional Counterpart

G. Wang, J. Si and J. Mi

Department of Energy & Resources Engineering
College of Engineering, Peking University, Beijing, 100871, P.R. China

Abstract

The present work numerically studies both characteristics of traditional combustion (TC) and MILD combustion (MILDC) of a premixed jet ($\text{CH}_4/\text{O}_2/\text{N}_2$) flame behind a conical bluff body and in hot coflow (6% O_2 +94% N_2 in volume). Here, MILD is the acronym for Moderate or Intense Low-oxygen Dilution. Calculations are performed at the jet Reynolds number of $Re = 14000$ using RANS modelling integrating with transported PDF and GRI-Mech 2.11. Both TC and MILDC modes can be established when initiating the bluff-body recirculation zone (BB-RZ) with relatively high (1700 K) and low (1250 K) temperatures. A lifted jet 'flame' stabilized by auto-ignition due to the hot (1350 K) coflow forms the MILDC while an expanded recirculation zone behind the bluff body, which serves as a stable ignition source, generates the TC flame. The temperature rise from combustion is much lower and chemical reactions are far weaker for the MILDC, so the reaction zone volume is much larger. Highly significantly, the MILDC produces extraordinarily low NO_x emission that is less than 5% of that from the TC.

Introduction

The MILD combustion is a new promising technology for both improving thermal efficiency and reducing pollution emissions of burning fossil fuels [1, 2]. Comparing to traditional combustion (TC), the temperature field is more uniform and flame is invisible in MILDC; so, it is also frequently called flameless oxidation (FLOX) [2]. Cavaliere and de Joannon [1] proposed the following two requirements for the establishment of MILDC: (i) the reactant temperature $> T_{ai}$ (auto-ignition temperature) prior to main combustion reactions and (ii) the temperature rise from combustion $< T_{ai}$. Internal or external dilution by hot exhaust gas usually plays a critical role in establishing MILD combustion.

Flame stabilization is a top issue in a practical combustion system. Previous works have extensively studied flame stabilization for turbulent jet flames [3-7]. Cabra et al. [3, 4] investigated the lifted H_2/N_2 and CH_4/air jet flame in a vitiated coflow burner (VCB). They found that the flame stabilization is a complicated process of mixing, ignition and flame propagation. Masri et al. [5] conducted detailed calculations on that flame using PDF method and concluded that auto-ignition dominates the flame stabilization process. The fuel jet is ignited spontaneously by entraining hot vitiated coflow and thus formed as a stabilized lifted flame. Dally et al. [6] experimentally examined a CH_4/H_2 jet flame in hot coflow (JHC), finding that MILDC is much more stable than TC. Oldenhof et al. [7] reported that the entrainment of ambient fluid is crucial in flame stabilization. The fuel jet entrains large amount of hot oxidant coflow and is then heated and diluted. The fuel temperature rises within the mixing process, then auto-ignition occurs and stabilized MILDC is established.

Bluff body (BB) is usually used to enhance the flame stability through a downstream recirculation zone (RZ). Reactants stay for a considerably long time in the BB-RZ and there a stable

flame is created [8], which continuously ignites oncoming reactants. Dally et al. [9, 10] investigated the flow and scalar fields and NO_x formation in the non-premixed jet flame. They concluded that the mixing between the air/fuel flow and the BB-RZ vortex is crucial to form a stabilized flame. NO_x is mainly generated either in the BB-RZ or just after the stagnation point. Tong et al. [11] reported that a BB mounted some distance above the annular channel exit can benefit flame stabilization.

Moreover, spark ignition is practically essential for turbulent BB flames. Noor et al. [12] found that the behaviour of flame stabilization highly depends on the ignition energy and spark location. These investigators showed that a BB cannot stabilize the traditional flame behind it when ignition fails with an insufficient spark energy. That is, the BB-RZ and sufficient heat source located in the RZ are both necessary for a stable traditional flame behind a BB. If there is a hot (temperature $> T_{ai}$) coflow present in their case, we postulate that their reactants will spontaneously ignite downstream of the BB and finally form a lifted 'flame' of MILDC. This postulation indeed has been confirmed by our numerical simulations.

This paper reports different MILDC and TC characteristics of the two methane flames behind a conical BB whose initial conditions for the premixed reactant jet and the surrounding coflow are identical. The aim is to quantify the differences between the MILDC and TC flames generated *under the same inlet and boundary conditions*, which has never been performed until now. Specifically, their flow and mixing processes, flame stabilizations, reaction zone characteristics, and NO_x distributions and emissions will be compared in this paper with discussion.

Numerical Setup

Present simulations are validated using the experimental results of Cabra et al. [4]. They investigated a premixed jet flame consisting of a central premixed CH_4/air jet with equivalent ratio (Φ_j) of 4.4 and a hot vitiated coflow of the combustion products of a lean H_2/air flame. Their jet exit velocity (U_j) and coflow velocity (U_c) are 100 m/s and 5.4 m/s, respectively. The jet diameter (d) is 4.57 mm, corresponding to a Reynolds number of $Re = 28000$. The temperatures of the central jet (T_j) and the hot coflow (T_c) are $T_j = 320$ K and $T_c = 1350$ K.

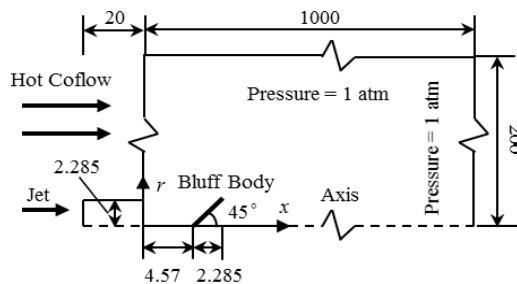


Figure 1. Schematic of the computational domain (unit in mm).

We use a different configuration for the present work where a conical bluff body is placed downstream at $x = 1d$ to stabilize

the flame, see Figure 1. U_J and U_C are reduced to 50 m/s and 1.0 m/s, respectively, to avoid blow-off. The coflow oxygen level is decreased to 6% to establish the lifted MILDC flame. The jet equivalent ratio (Φ_J) is varied from 0.8 to 1.2 to investigate lean and rich flames. The mole fraction of CH₄ (X_{CH_4}) is constant for different Φ_J to keep the same power rate ($P = 4.9$ kW). The inlet conditions are summarized in Table 1.

Parameter	Central Jet	Coflow
T (K)	$T_J = 320$	$T_C = 1250$
U (m/s)	$U_J = 50.0$	$U_C = 1.0$
X_{O_2}	0.417, 0.333, 0.278	0.06
X_{N_2}	0.416, 0.500, 0.555	0.94
X_{CH_4}	0.167	0.00
Φ	$\Phi_J = 0.8, 1.0, 1.2$	----

Table 1. Inlet conditions for the calculated cases.

Considering the symmetry of the calculated configuration, we employed a simplified two-dimensional (2D) computational model. The computational domain, see Fig. 1, spans 1000 mm (about $219d$) and 200 mm (about $44d$) in the axial and radial directions, respectively. A stretched structured grid with about 20,000 cells is used, with the minimum and maximum grid sizes of $0.03d$ and $2.2d$, respectively.

The present simulations use the commercial software ANSYS Fluent 17.2 to solve the transport equations, together with composition PDF model and full chemistry mechanism of GRI-Mech 2.11. The standard $k-\epsilon$ model is adopted to model the turbulent flows, in which $C_{1\epsilon}$ is modified to 1.6 as in [13, 14]. The discrete ordinate (DO) model together with the weighted sum of grey gas model (WSGGM) is employed as the radiation model. The composition PDF model with a detailed chemical kinetics mechanism (GRI-Mech 2.11 [15]) is used to simulate the turbulent-chemistry interaction. The modified Curl model [16] is used to emulate the particle mixing process, with 20 particles (suggested in [5]) in each grid cell. To reduce the computational cost, the In-Situ Adaptive Tabulation (ISAT) method by Pope [17] is used and the ISAT error tolerance is set to be 5×10^{-6} according to Masri et al. [5]. The SIMPLE scheme is adopted to solve pressure-velocity coupling and the second order upwind scheme is applied for spatial discretization. Convergence is reached at the residuals $< 10^{-6}$ for energy and radiation equations and $< 10^{-5}$ for other equations.

Results and Discussion

Experimental Validation

Present simulations are validated by the experimental premixed CH₄/air jet flame [4]. Figure 2 demonstrates the centreline simulations and measurements of the Favre-averaged temperature ($\langle T \rangle$) and its root-mean-square (RMS) value (T'), and mass fractions ($\langle Y_{O_2} \rangle$, $\langle Y_{CO_2} \rangle$, $\langle Y_{CO} \rangle$ and $\langle Y_{H_2} \rangle$). Overall, the predictions of the temperature and species concentrations agree well with the experimental data, allowing some quantitative discrepancies for the intermediate species CO and H₂. Note that the simulation overvalues the centreline $\langle Y_{CO} \rangle$ and $\langle Y_{H_2} \rangle$. So, it is appropriate for the study to use the RANS modelling together with the PDF model and GRI-Mech 2.11.

Establishments of the MILDC and TC

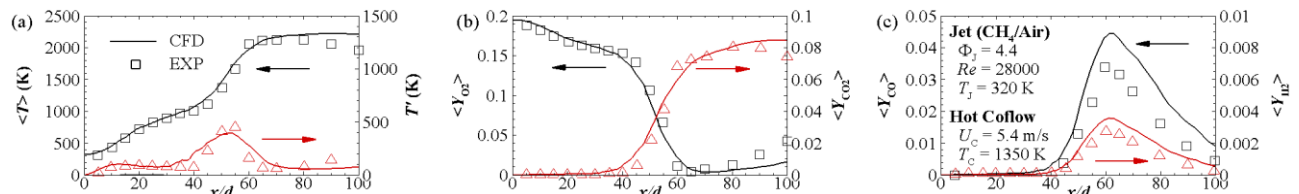


Figure 2. Comparison between numerical and experimental [4] results of centreline Favre-averaged temperature and species concentrations: (a) $\langle T \rangle$ and T' ; (b) $\langle Y_{O_2} \rangle$ and $\langle Y_{CO_2} \rangle$; (c) $\langle Y_{CO} \rangle$ and $\langle Y_{H_2} \rangle$.

High temperature patching is presently used to mimic spark ignition. For the unreacted flow, set a high temperature initially in the BB-RZ. When the initiated temperature is not high enough (1250 K) to sustain the ignited flame behind the BB, the premixed reactants will be flushed away downstream. Then they will be heated and diluted by the hot vitiated coflow at $T_C = 1250$ K and form a lifted flame far downstream through auto-ignition (Figure 3). However, if the temperature is sufficiently high (1700 K) behind the bluff body so that the 'spark' ignition is successful, then the flame will be stabilized there, forming an expanded recirculation zone flame (Figure 3).

Figure 3 presents the Favre-averaged temperature ($\langle T \rangle$) for the two flames with $\Phi_J = 1.0$. When ignition with the temperature of 1250 K, the flame is lifted and stabilized at $x \geq 35d$ in the jet mixing layer, see the upper half of the figure. Because of the dilution of the low-oxygen coflow, the flame temperature is depressed with peak value of 1787 K, only 537 K higher than the coflow temperature, so it is in the MILDC regime. For the higher ignition temperature of 1700 K, a stable flame develops immediately downstream from, and is also stabilized by, the BB. This is a typical traditional combustion (TC) flame with the peak temperature of 2587.2 K.

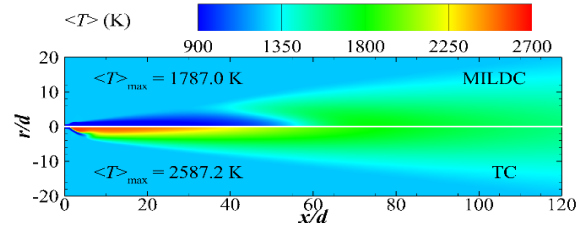


Figure 3. Centre-plane contours of Favre-averaged temperature ($\langle T \rangle$) under the MILDC (upper) and TC (lower) regimes.

In summary, under the identical inlet conditions of the jet and coflow, both TC and MILDC regimes for the premixed flame can be established by initiating the ignition with different temperatures. Next, we will examine below the differences of these two flames in their flow and mixing processes, reaction zone characteristics and NO_x formations and emissions.

Flow and Mixing Fields

Figure 4 presents the centre-plane contours of the axial velocity (U_x) and Favre-averaged mixture fraction ($\langle Z \rangle$, calculated using Bilger's formula [18]) for the MILDC and TC cases with $\Phi_J = 1.0$. As clearly shown in Figure 4a, a successful ignition for the TC significantly changes the BB downstream flow field. The BB-RZ expands substantially, which agrees with the result of Tong et al. [11]. In the TC case, the mixture burns in the BB-RZ, growing the local temperature. Therefore, the fluid density decreases and the velocity is thus elevated, enlarging the BB-RZ size. The peak back-flow velocity is 32 m/s in the TC case, much higher than that (24 m/s) in the MILDC case.

The mixing fields in the two cases are demonstrated in Figure 4b. The white dashed line indicates the position where $\langle Z \rangle = 0.8$. The mixing process is greatly intensified in the TC case because of the strong turbulent mixing in the BB-RZ. The premixed jet is simultaneously diluted by both the combustion products from the BB-RZ and the hot vitiated coflow outside.

As a consequence, $\langle Z \rangle$ decreases quickly with increasing x . However, for the MILDC, combustion reactions do not occur in the BB-RZ, so the premixed jet is diluted only by the co-flowing hot and low-O₂ mixture, which is a slow process. Hence, the mixture fraction remains high for a long distance.

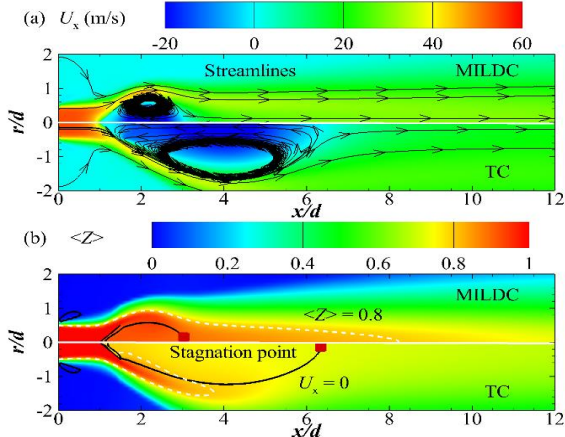


Figure 4. Centre-plane contours of the axial velocity (U_x) and Favre-averaged mixture fraction ($\langle Z \rangle$) under the MILDC and TC regimes.

Reaction Zone Characteristics

Following the work of Mei et al. [14], we define $R_{CO} = 0.05$ for the boundary of the reaction zone where

$$R_{CO} = \langle Y_{CO} \rangle / \langle Y_{CO} \rangle_{\max} \quad (1)$$

and $\langle Y_{CO} \rangle_{\max}$ is the maximum Favre-averaged mass fraction of CO in the whole computation domain. Figure 5 demonstrates the centre-plane contours of Favre-averaged CO and OH mass fractions ($\langle Y_{CO} \rangle$ and $\langle Y_{OH} \rangle$) for the MILDC and TC with $\Phi_J = 1.0$. Logarithm is used to highlight low values of $\langle Y_{CO} \rangle$ and $\langle Y_{OH} \rangle$ in the MILDC case. The black solid line represents the position where $R_{CO} = 0.05$. For both cases, CO mainly distributes within the defined reaction zone while OH extends farther downstream, which agrees well with previous studies, e.g. [14]. Moreover, CO appears earlier than OH and the temperature rise. For the MILDC case, CO and OH levels are much lower than in the TC case by 1-2 orders of magnitude, indicating that combustion reactions take place much more rapidly in the TC than in the MILDC. The locations of the peak $\langle Y_{CO} \rangle$ and $\langle Y_{OH} \rangle$ also vary from within the jet mixing layer for the MILDC case to the inside of the BB-RZ for the TC case.

The flow structure is expected to be very different for the two cases and so are the reaction zone characteristics. It is evident that the reaction zone is larger in the MILDC than TC case. The length is $> 95d$ for the MILDC and about $45d$ for the TC.

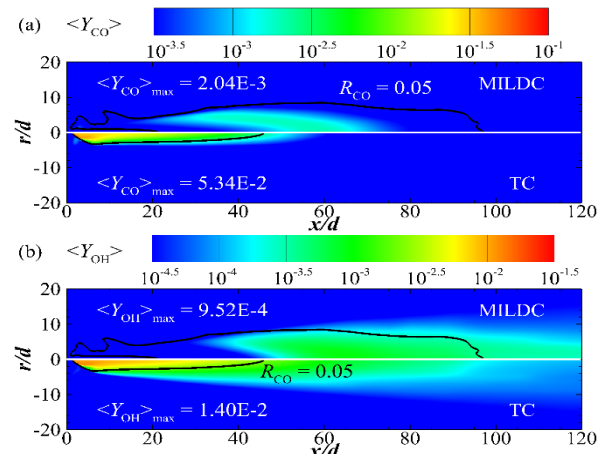


Figure 5. Center-plane contours of Favre-averaged mass fractions of (a) CO and (b) OH ($\langle Y_{CO} \rangle$ and $\langle Y_{OH} \rangle$) under the MILDC and TC regimes.

The reaction is drastic in the TC case and the premixed reactants burn out rapidly in and after the BB-RZ. For the MILDC case, the premixed jet is well diluted by the hot coflow before main reactions occur at moderate rates. Therefore, the reaction zone is enlarged substantially.

To quantify the size of the reaction zone, its volume (V_R) is calculated and shown in Figure 6. For the MILDC case, V_R is about eighteen times as that for the TC case. As the jet equivalent ratio (Φ_J) increases, the oxygen level in the premixed jet reduces, so the fuel needs more oxygen from the hot coflow to burn out. Hence, V_R increases as Φ_J increases. On the other hand, as Φ_J increases, the ratio $V_{R,MILDC}/V_{R,TC}$ decreases. At low $\Phi_J < 1.0$, the fuel burns completely in the BB-RZ for the TC case. For $\Phi_J > 1.0$, as Φ_J increases, the oxygen in the premixed jet is not sufficient and part of the fuel has to react with the oxygen from the coflow. This behaviour is like the MILDC and becomes dominant as Φ_J increases further.

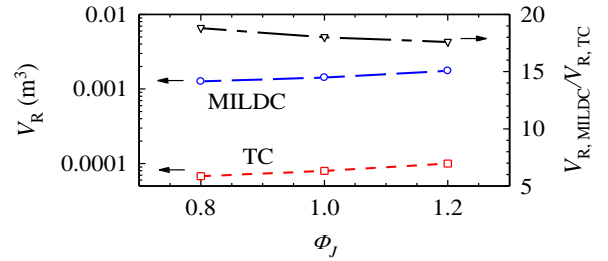


Figure 6. Reaction zone volume (V_R) versus jet equivalent ratio (Φ_J) in the MILDC and TC cases.

NO_x Distribution and Emission

Figure 7 shows the centre-plane contours of the Favre-averaged mass fraction of NO_x (Y_{NO_x}) for the MILDC and TC cases at $\Phi_J = 1.0$. For the MILDC case, NO_x begins to form at $x \geq 35d$. In the TC flame, NO_x mainly forms in the BB-RZ and just after the stagnation point, consistent with the measurement of Dally et al. [10]. Moreover, in the MILDC case, Y_{NO_x} is much less than that in the TC case by 2-3 orders of magnitude, due to greatly reduced combustion temperature. When temperature is higher than 1800K, NO_x begins to accumulate rapidly [19].

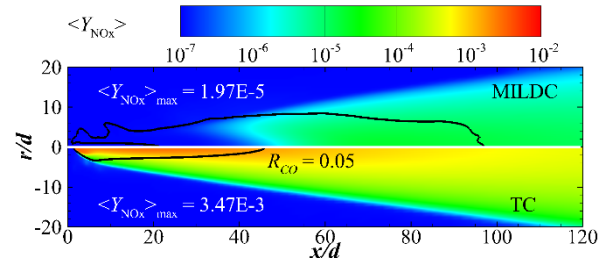


Figure 7. Center-plane contours of Favre-averaged mass fraction of NO_x (Y_{NO_x}) under the MILDC and TC regimes.

The NO_x emissions can be measured by the emission index of NO_x (EI_{NO_x}) [19] defined as

$$EI_{NO_x} = \frac{m_{NO_x, \text{emitted}}}{m_{F, \text{burned}}} \times 1000 \quad (2)$$

where m_i is the mass flux of i th species. We calculate EI_{NO_x} at the end of the reaction zone and that of the computational domain. Figure 8 demonstrates the results. Evidently, the NO_x emission from the MILDC is less than 5% of that from the TC. As Φ_J increases, EI_{NO_x} gradually decreases in both cases owing to the reductions of temperature and local oxygen. Moreover, the NO_x emission remains to increase from the end of the reaction zone to the end of computational domain, as high-temperature N₂ and O₂ from the coflow react with each other to continuously form NO_x downstream of the reaction zone.

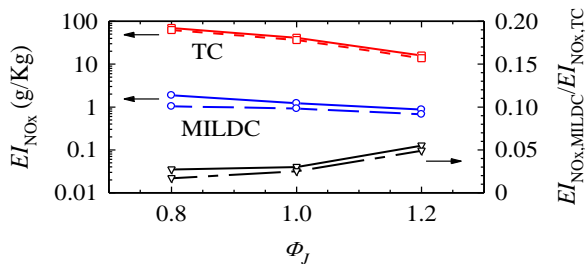


Figure 8. NO_x emission index (EI_{NO_x}) at the ends of the reaction zone (dashed lines) and the computational domain (solid lines) in the MILDC and TC cases.

Conclusions

The present work has calculated and analysed the traditional and MILDC combustion characteristics in a premixed jet flame behind a conical bluff body. These two distinct flames can be established by initiating the ignition process with different temperatures in the BB-RZ *under the same inlet and boundary conditions*. More specifically, we have found the following differences:

- (1) **Flame stabilization mechanism.** For the MILDC case, the premixed jet is heated and diluted by the hot coflow. The flame is then stabilized and lifted up by auto-ignition. However, in the TC case, there is a stabilized pilot flame in the recirculation zone that continuously ignites the oncoming reactants and forms a stable conventional flame.
- (2) **Flow and mixing process.** The combustion behind the bluff body accelerates the premixed jet and enlarges the recirculation zone in the TC case comparing to the MILDC case. Moreover, the mixing process is greatly intensified by the strong turbulence in the recirculation zone and so the mixture fraction decreases rapidly in the TC case.
- (3) **Reaction zone characteristics.** In the MILDC flame, the temperature rise due to combustion is substantially lower and combustion reactions are weaker. So, the reaction zone is significantly larger than that in the TC flame. As Φ_j increases, the reaction zone increases in size for both flames.
- (4) **NO_x formation and emission.** NO_x forms downstream of the flame lift-off height in the MILDC flame while the NO_x formation mainly occurs in the recirculation zone and just after the stagnation point in the TC flame. It is important to note that the MILDC combustion produces extraordinarily low NO_x emission, only 5% or less of that from the traditional combustion.

Acknowledgements

The authors greatly acknowledge the support of Natural Science Foundation of China (No. 51776003) and High-Performance Computing Platform of Peking University.

References

- [1] Cavaliere, A. & de Joannon, M., Mild Combustion, *Prog. Energy Combust. Sci.*, **30** (4), 2004, 329-366.
- [2] Wünnig, J.A. & Wünnig, J.G., Flameless Oxidation to Reduce Thermal NO -formation, *Prog. Energy Combust. Sci.*, **23** (1), 1997, 81-94.
- [3] Cabra, R., Myhrvold, T., Chen, J.-Y., Dibble, R.W., Karpetis, A.N. & Barlow, R.S., Simultaneous Laser Raman-Rayleigh-LIF Measurements and Numerical Modeling Results of a Lifted Turbulent H_2/N_2 Jet Flame in

a Vitiated Coflow, *Proc. Combust. Inst.*, **29** (2), 2002, 1881-1888.

- [4] Cabra, R., Chen, J.-Y., Dibble, R.W., Karpetis, A.N. & Barlow, R.S., Lifted Methane-air Jet Flames in a Vitiated Coflow, *Combust. Flame*, **143** (4), 2005, 491-506.
- [5] Masri, A.R., Cao, R., Pope, S.B. & Goldin, G.M., PDF Calculations of Turbulent Lifted Flames of H_2/N_2 Fuel Issuing into a Vitiated Co-flow, *Combust. Theory Modell.*, **8** (1), 2004, 1-22.
- [6] Dally, B.B., Karpetis, A.N. & Barlow, R.S., Structure of Turbulent Non-premixed Jet Flames in a Diluted Hot Coflow, *Proc. Combust. Inst.*, **29** (1), 2002, 1147-1154.
- [7] Oldenhof, E., Tummers, M.J., van Veen, E.H. & Roekaerts, D.J.E.M., Role of Entrainment in the Stabilisation of Jet-in-hot-coflow Flames, *Combust. Flame*, **158** (8), 2011, 1553-1563.
- [8] Kundu, K.M., Banerjee, D. & Bhaduri, D., Theoretical Analysis on Flame Stabilization by a Bluff-Body, *Combust. Sci. Tech.*, **17** (3-4), 1977, 153-162.
- [9] Dally, B.B., Masri, A.R., Barlow, R.S. & Fiechtner, G.J., Instantaneous and Mean Compositional Structure of Bluff-body Stabilized Nonpremixed Flames, *Combust. Flame*, **114** (1-2), 1998, 119-148.
- [10] Dally, B.B., Masri, A.R., Barlow, R.S., Fiechtner, G.J. & Fletcher, D.F., Measurements of NO in Turbulent Non-premixed Flames Stabilized on a Bluff Body, *Proc. Combust. Inst.*, **26** (2), 1996, 2191-2197.
- [11] Tong, Y., Liu, X., Chen, S., Li, Z. & Klingmann, J., Effects of the Position of a Bluff-body on the Diffusion Flames: A Combined Experimental and Numerical Study, *Appl. Therm. Eng.*, **131**, 2018, 507-521.
- [12] Noor, M.M., Wandel, A.P. & Yusaf, T., Analysis of Recirculation zone and Ignition Position of Non-premixed Bluff-body for Biogas MILDC Combustion, *Int. J. Automot. Mech. Eng.*, **8** (1), 2013, 1176-1186.
- [13] Dally, B.B., Fletcher, D.F. & Masri, A.R., Flow and Mixing Fields of Turbulent Bluff-body Jets and Flames, *Combust. Theory Modell.*, **2**(2), 1998, 193-219.
- [14] Mei, Z., Mi, J., Wang, F., Li, P. & Zhang, J., Chemical Flame Length of a Methane Jet into Oxidant Stream, *Flow, Turb. Combust.*, **94** (4), 2015, 767-794.
- [15] Bowman, C.T., Hanson, R.K., Davidson, D.F., Jr., Gardiner, W.C., Lissianski, V., Smith, G.P., Golden, D.M., Frenklach, M., & Goldenberg, M., available at http://www.me.berkeley.edu/gri_mech/.
- [16] Nooren, P.A., Wouters, H.A., Peeters, T.W.J., Roekaerts, D., Maas, U. & Schmidt, D., Monte Carlo PDF Modelling of a Turbulent Natural-gas Diffusion Flame, *Combust. Theory Modell.*, **1**(1), 1997, 79-96.
- [17] Pope, S.B., Computationally Efficient Implementation of Combustion Chemistry Using In Situ Adaptive Tabulation, *Combust. Theory Modell.*, **1**(1), 1997, 41-63.
- [18] Bilger, R.W., Stårner, S.H. & Kee, R.J., On Reduced Mechanisms for Methane-air Combustion in Nonpremixed Flames, *Combust. Flame*, **80** (2), 1990, 135-149.
- [19] Turns, S.R., *An Introduction to Combustion*, New York: McGraw-hill, 1996.